Journal of Thermal Analysis and Calorimetry (2021) 146:153–164
https://doi.org/10.1007/s10973-020-10420-8

Experimental study on the synergistic flame retardant effect of bio-based magnesium phytate and rice husk ash on epoxy resins

Yanying Xu[1] · Jindu Li[1] · Ruiqing Shen[2] · Zhi Wang[1] · Po Hu[1] · Qingsheng Wang[2]

Received: 15 June 2020 / Accepted: 18 November 2020 / Published online: 3 January 2021

Abstract

Bio-based flame retardant magnesium phytate (Mg-Phyt) was synthesized by a facile chelation reaction and characterized. The feasibility of Mg-Phyt as flame retardant for epoxy resins was studied. In order to enhance its flame retardancy, the synergistic flame retardancy between Mg-Phyt and agricultural waste material rice husk ash (RHS) and the synergistic effects of different ratios of these two were investigated. The results show that the addition of 10 mass% Mg-Phyt can reduce the thermal decomposition rate and achieve good flame retardant performance for epoxy resins. Furthermore, the combination of Mg-Phyt with RHS can have a synergistic flame retardant effect. Among them, the synergistic effect of 5 mass% Mg-Phyt and 5 mass% RHS is the best when the two substances are added into epoxy resins. More specifically, compared to pure epoxy resins, the peak heat release rate, total heat release, peak smoke production rate, and total smoke release of epoxy resins with 5 mass% Mg-Phyt and 5 mass% RHS are reduced remarkably by 28.6%, 10.6%, 33.0%, and 7.8%, respectively. The burning rate is also reduced by 42.4%. During the combustion process, this synergistic flame retardant effect is attributed to the formation of a compact silica-rich char layer containing Si–P and P–O–C structures with strong thermal stability to hinder the heat transfer into the epoxy resins substrate and reduce flammable gas emission, so that a better flame retardancy and smoke suppression of epoxy resins can be attained.

Keywords Epoxy resins · Bio-based flame retardants · Magnesium phytate · Rice husk ash · Synergistic flame retardant effect

Introduction

Epoxy resins (EP) have excellent mechanical, electrical, and agglutinate properties, and they are widely used in the engineering field as coatings, composite materials, casting materials, and adhesives [1–4]. However, the high flammability of epoxy resins is a big concern to life safety and property safety during applications [5, 6]. To control the fire hazard of epoxy resins in applications, improving the flame retardancy is essential, in which flame retardants are usually embedded into epoxy resins to improve their fire safety. Among the flame retardants that have been developed, halogen-containing flame retardants have shown excellent performance, but their applications have been legislatively prohibited due to severe health and environmental concerns [7]. In recent years, more interest has been focused on the research and development of halogen-free flame retardants [8, 9]. Some halogen-free flame retardants such as phosphorus-based, nitrogen-based, silicon-based, boron-based, carbon nanotubes, layered double hydroxides, and montmorillonite have been widely used in polymers [10–16]. Phosphorus-based flame retardants act by trapping free radicals (H· or OH·) in the gaseous phase and facilitating the formation of char in the condensed phase [17–19]. Moreover, most phosphorus-based flame retardants have the advantages of high efficiency and low cost [20].

In recent years, 9,10-dihydro-9-oxa-10-phosphaphenanthrene-10-oxide (DOPO), ammonium polyphosphate (APP), and their derivatives are common types of phosphorus-based flame retardants, which have been used to improve the fire safety of epoxy resins [21–25]. Compared with

✉ Qingsheng Wang
qwang@tamu.edu

[1] Liaoning Key Laboratory of Aircraft Safety and Airworthiness, Shenyang Aerospace University, Shenyang 110136, China

[2] Mary Kay O'Connor Process Safety Center, Artie McFerrin Department of Chemical Engineering, Texas A&M University, College Station, TX 77843, USA

these chemicals, bio-based flame retardants can be derived from green feedstocks and are environmentally friendly [26]. However, the study of bio-based flame retardant for epoxy resins is very limited. To develop environmentally friendly and highly efficient flame retardants for epoxy resins, the study of bio-based phosphorus-containing flame retardants is of great importance. The phytic acid (inositol hexaphosphate) present in cereals and beans is non-toxic, shows good biocompatibility, and has high phosphorus content. The phytic acid has strong chelation and can form complexes (metallic phytate) with metal cation [27, 28]. So far, the phytic acid has been found to have great potential as flame retardant for polymers, but there are a few applications of metallic phytate as flame retardant for polymer, especially for eposy resins [27]. For example, Costesab et al. [29] studied the potential flame retardant effect of different metallic phytates (Na-phyt, Al-phyt, Fe-phyt, La-phyt) on PLA, and found that Al-phyt could significantly reduce the forced burning intensity of PLA. Yang et al. [27] used calcium magnesium phytate and carbon nanotubes as flame retardants for polylactic acid (PLA) and achieved considerable reduction in the burning intensity. Metallic phytates synthesized by direct precipitation method were used as flame retardants for PVC, and the results showed that PVC with 15 mass% metallic phytate had good carbonization [28]. Rice husk ash (RHS) is an agricultural waste material that could be useless because of its limited advanced applications [30]. It is cheap and has high silicon content [30–32], which has been used as a bio-based flame retardant to improve the flame retardancy of polymers. Almiron et al. [33] found that RHS and phosphorus-based flame retardants (APP and pentaerythritol) have a synergistic effect on polypropylene. As a bio-halogen-free flame retardant, melamine phosphate-modified lignin (MAP-lignin) and RHS can significantly increase char residue of poly(3-hydroxybutyrate-co-4-hydroxybutyrate) (P34HB) biocomposites and their flame retardant performance can also be improved by adding 30 mass% MAP-lignin and 5 mass% RHS [34]. Since metallic phytate is non-toxic and has high phosphorus content, and the synergistic effect may be brought by the elements of phosphorus and silicon on improving the thermal stability and flame retardancy of epoxy resins [35], metallic phytate and RHS are considered as potential bio-based flame retardants for epoxy resins.

To find an environmentally friendly and highly efficient flame retardant system for epoxy resins, the feasibility of Mg-Phyt as a bio-based phosphorus-containing flame retardant for epoxy resins was studied. Furthermore, to improve the flame retardant effect, the synergistic effect of Mg-Phyt and RHS on epoxy resins and the influence of the ratio of these two on the flame retardant performance were also studied. In this study, Fourier Transform Infrared Spectroscopy (FTIR) was used to investigate the structures of Mg-Phyt and RHS. Mg-Phyt and RHS were added into epoxy resins separately or in combination to form different composites. Thermogravimetric analysis (TGA), cone calorimeter, Underwriter Laboratories 94 (UL-94), and limiting oxygen index (LOI) tests were used to comprehensively study the thermal properties and flame retardant properties of the epoxy resin composites, coupling with Scanning Electron Microscopy (SEM) and X-ray Photoelectron Spectroscopy (XPS).

Experimental

Materials

Bisphenol-A (DEGBA) epoxy resins were supplied by Blue Star Synthetic Material Co., Ltd., China. The curing agent (2-Ethyl-4-methylimidazole) was purchased from Shikoku Chemical Co., Ltd., Japan. Sodium phytate (99 mass%) and Magnesium chloride were purchased from the Sinopharm Chemical Reagent Co., Ltd., China. The raw material of rice hush was purchased from the market and rice hush ash (RHS) was obtained from rice hush by grinding and screening.

Preparation of magnesium phytate

Mg-Phyt was obtained by mixing a 0.5 mol L^{-1} $MgCl_2{\cdot}6H_2O$ aqueous solution with another 0.1 mol L^{-1} Na-Phyt aqueous solution. The system was refluxed at 100 °C for 1 h under constant mechanical stirring to obtain Mg-Phyt precipitate [29]. Then, the precipitated Mg-Phyt was washed by centrifugation with deionized water for five times. Last, Mg-Phyt was dried at 105 °C for 2 h.

Preparation of samples

The samples were prepared as shown in Table 1, in which the mass fraction of different components is given. During the preparation, epoxy resins, Mg-Phyt, and RHS were weighed accurately according to the mass fraction and then mixed with a mechanical stirrer at 500 rpm and 90 °C until

Table 1 The mass fraction of each component in the samples

Samples	Epoxy resins/mass%	Mg-Phyt/mass%	RHS/mass%
EP	100	0	0
EP-M10-R0	90	10	0
EP-M0-R10	90	0	10
EP-M2.5-R7.5	90	2.5	7.5
EP-M5-R5	90	5	5
EP-M7.5-R2.5	90	7.5	2.5

they were uniformly mixed. With a mass ratio to epoxy resins of 5: 100, imidazole (curing agent) was added into the treated epoxy resins while the stirring was continued to obtain a uniform mixture. Then, the mixture was poured into the mold. The material in the mold was cured at 90 °C for 4 h.

Characterizations

FTIR spectroscopy analysis was performed using a Nicolet 380 spectrophotometer (Thermo Scientific) at a spectral range of 4000–400 cm^{-1}, with a resolution of 4 cm^{-1} and the number of scans of 32. Thermogravimetric analysis (TGA) was conducted using the DTG-60 (AH) thermal analyzer (Japan) at the temperature range from 35 °C to 800 °C at a heating rate of 20 °C min^{-1} under a nitrogen atmosphere with a flow rate of 50 mL min^{-1}. The flame retardancy of the samples was tested in a horizontal orientation using the FTT-CONE-228 cone calorimeter (England) under the irradiance heat flux of 35 kW m^{-2} with a grid. Cone calorimeter tests were performed according to ISO 5660-1 protocol. The UL 94 tests were performed according to IEC 60695-11-10:2003 using a horizontal and vertical burning instrument (CZF-5, China). Limiting Oxygen Index (LOI) was tested according to ISO 4589-3 with FTT-OL-1402072 LOI test instrument (England). The morphology of char residues after the cone calorimeter test was characterized by a scanning electron microscope (SEM) on a Hitachi SU3500 SEM (Tokyo, Japan) with an acceleration voltage of 10 kV. X-ray Photoelectron Spectroscopy (XPS) was measured on an ESCALAB 250Xi X-ray photoelectron spectrometer (Thermo Scientific Company, USA) with an Al Kα X-ray source to study the chemical structure of char residues. And the software XPSPEAK was used to peak-differentiating and imitating.

Results and discussion

Characterization of Mg-Phyt and RHS

The FTIR was performed to demonstrate the successful synthesis of Mg-Phyt. Figure 1a shows the FTIR spectra of Na-Phyt and Mg-Phyt. Figure 2 shows the structural formula of Mg-Phyt. Na-Phyt and Mg-Phyt both show a wide absorption band at 3394 cm^{-1} and a weak absorption band at 1646 cm^{-1}. The bands observed at 3394 cm^{-1} and 1646 cm^{-1} are attributed to the stretching vibration mode of O-H and the twisting vibration mode of the H–O–H, respectively. Because the samples were dried at 105 °C for 2 h, Na-Phyt and Mg-Phyt only contain crystalline or adsorbed water molecules [36, 37]. The absorption peak near 1400 cm^{-1}

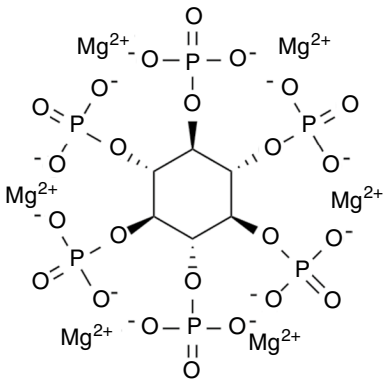

Fig. 2 The molecular structure of Mg-Phyt

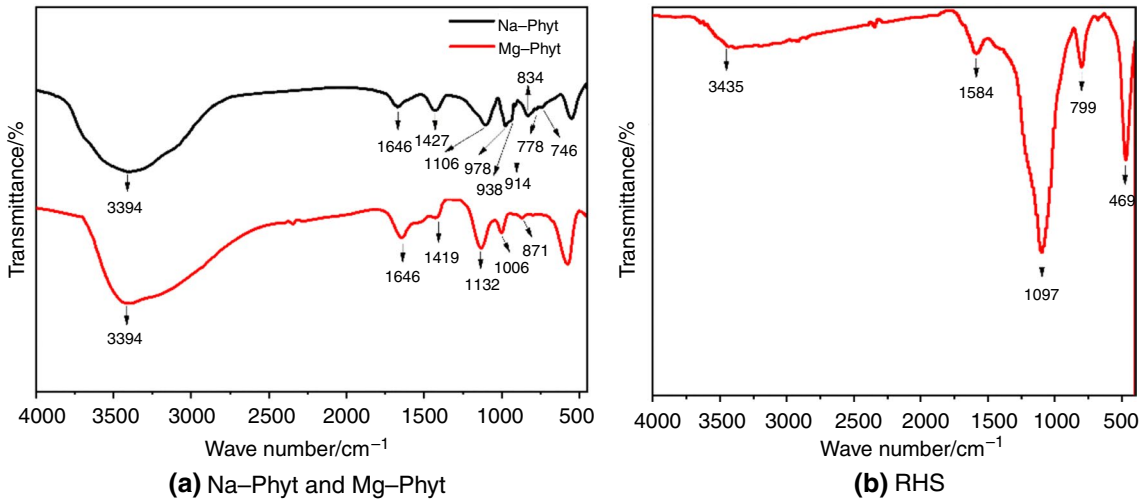

Fig. 1 FTIR spectra of Mg-Phyt and RHS

is considered to be the stretching vibration of the P=O bond [38]. The sharp band of Na-Phyt at 1106, 978, and 834 cm^{-1} were shifted to 1132, 1006, 871 cm^{-1} with Mg-Phyt. The spectrum of Na-Phyt shows triplet bands at 978, 938, and 914 cm^{-1}, and another triplet bands at 834, 778, and 746 cm^{-1}, but there are no triplet bands in Mg-Phyt. This indicates that the structure of Mg-Phyt is different from that of Na-Phyt. Furthermore, the characteristic infrared spectra of Mg-Phyt is from 1200 to 700 cm^{-1}, and there are three absorption peaks in this characteristic infrared spectra [37]. The absorption peaks at 1132 cm^{-1}, 1006 cm^{-1}, and 871 cm^{-1} are the same as the characteristic infrared spectra of Mg-Phyt, demonstrating that Mg-Phyt has been successfully synthesized.

Figure 1b shows the FTIR spectra of RHS. The main component of rice husk ash is silica, and the three important bands for identifying SiO_2 is seen in Fig. 1b. The band at 1097 cm^{-1} is attributed to the asymmetrical stretching mode of the Si–O-Si group; the absorption peaks at 799 cm^{-1} and 469 cm^{-1} are attributed to the bending vibration mode and the rocking mode of the Si–O group, respectively [33].

Thermal Analysis

The TGA and DTG (the first derivative curve of TGA, which shows the mass loss rate relative to temperature or time) curves of the samples in nitrogen are shown in Fig. 3. The initial thermal decomposition temperature ($T_{5\%}$), the maximum thermal decomposition temperature (T_{max}), and the char residues at 800 °C are shown in Table 2. It can be seen that EP shows one main step of decomposition in nitrogen. This decomposition step is in the temperature range of 350–500 °C, resulting from the decomposition of epoxy resins [39]. This step corresponds to an obvious DTG peak at 454 °C. When RHS was added, EP-M0-R10 still shows one main step of decomposition, because RHS has high thermal stability over this temperature range [40], so that this main step is also related to the decomposition of epoxy resins. However, when Mg-Phyt was added or Mg-Phyt and RHS were both added, there are two main steps of decomposition in nitrogen. The first step occurred in the temperature range of 150–250 °C, and the second decomposition step occurred in the temperature range of 350–500 °C. The temperature ranges of the second decomposition step of EP-M10-R0, EP-M2.5-R7.5, EP-M5-R5 and EP-M7.5-R2.5 are close to that of EP and EP-M0-R10, so that the second decomposition step of EP-M10-R0, EP-M2.5-R7.5, EP-M5-R5, and EP-M7.5-R2.5 is the decomposition of epoxy resins. Thus, the first decomposition step in the temperature range of 150–250 °C is ascribed to the decomposition of Mg-Phyt.

Table 2 The initial thermal decomposition temperature ($T_{5\%}$), the temperature at the maximum thermal decomposition rate (T_{max}), and the char residues at 800 °C

Samples	$T_{5\%}$/°C	T_{max}/°C	Char residues/mass%	Peak decomposition rate/% $°C^{-1}$
EP	416	454	10.68	1.344
EP-M10-R0	400	440	13.59	1.207
EP-M0-R10	435	465	19.69	1.125
EP-M2.5-R7.5	413	457	18.99	0.943
EP-M5-R5	409	451	16.22	0.939
EP-M7.5-R2.5	402	446	15.74	0.952

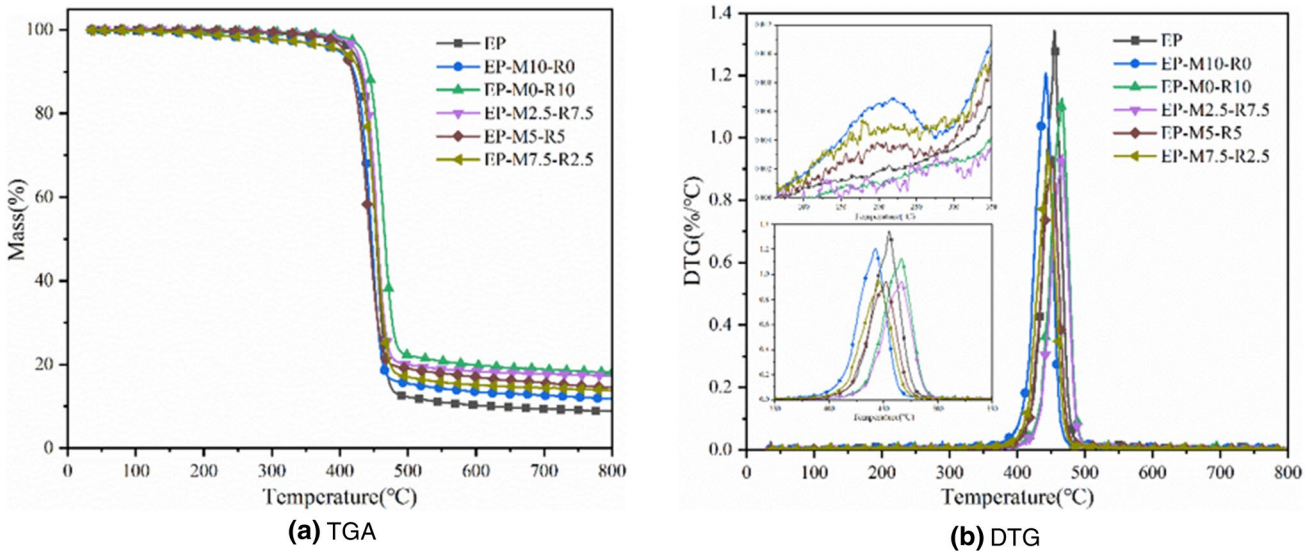

Fig. 3 The TGA and DTG curves of the samples in nitrogen

It can be seen that $T_{5\%}$ decreases from 416 °C for EP to 400 °C for EP-M10-R0, which occurs because Mg-Phyt begins its decomposition before epoxy resins to promote the formation of the char layer, and this behavior is necessary to protect epoxy resins from further decomposition [33]. Therefore, the decomposition rate of EP-M10-R0 is lower than EP. The T_{max} follows a similar trend to $T_{5\%}$, decreasing from 454 °C for EP to 440 °C for EP-M10-R0. Besides, the char residues of EP are 10.68%, while that of EP-M10-R0 is 13.59%, which indicates that the addition of Mg-Phyt is beneficial to the char formation of epoxy resins. $T_{5\%}$ of EP-M0-R10 increases to 435 °C due to the presence of silica from RHS, which can contribute to increasing the thermal decomposition temperature of epoxy resins [41]. With the increase in RHS content, $T_{5\%}$ and T_{max} of all samples increased. Therefore, when Mg-Phyt and RHS were added to epoxy resins together, the initial thermal decomposition temperature of epoxy resins is all higher than EP-M10-R0, but these initial thermal decomposition temperatures are still lower than EP. This means that Mg-Phyt can still decompose in advance to prevent the decomposition of epoxy resins. The combination of Mg-Phyt and RHS leads to a further reduction in the decomposition rate, for example, the peak decomposition rate of EP-M5-R5 is 0.939% $°C^{-1}$, which is lower than EP-M10-R0 and EP-M0-R10, indicating that the synergism took place between Mg-Phyt and RHS to decrease the decomposition rate. With the addition of RHS, the char residue was higher than that in which Mg-Phyt was added alone. Furthermore, the ratio of Mg-Phyt and RHS has some slight influence on the synergistic effect. When the mass ratio of Mg-Phyt and RHS is 5:5, the thermal decomposition rate decreases the most and the synergistic effect is slightly better.

In conclusion, the addition of Mg-Phyt slightly decreases the initial thermal decomposition temperature of epoxy resins, but it can slow down the decomposition rate of epoxy resins. The combination of Mg-Phyt and RHS leads to a synergistic effect in reducing the decomposition rate of epoxy resins, and the mass ratio of Mg-Phyt and RHS in 5: 5 can have a slightly better synergistic effect. It is also interesting to note that RHS plays a great role in the increase of $T_{5\%}$, T_{max}, and char residues.

Cone calorimeter tests

The cone calorimeter is the most versatile bench-scale instrument for measuring the reaction-to-fire properties of combustible materials [42]. Figure 4a, b shows the variation of the heat release rate (HRR) and smoke production rate (SPR) with time during the test. Figure 5 shows the peak heat release rate (pHRR), total heat release (THR), peak smoke production rate (pSPR), total smoke release (TSR) of the samples, and the rate of reduction compared to EP. Table 3 shows the cone calorimeter data for each sample at the irradiance heat flux of 35 kW m^{-2}.

It is seen from Table 3 that EP has intense flammability, which was ignited at about 124 s. From the combustion, a large amount of heat was released. Compared with EP, after the flame retardant was added, the times to ignition (TTI) of samples were all delayed, but the difference was small. With the increase in RHS content, the delay of ignition is more significant, which indicates that RHS is conducive to the delay of ignition time. In addition, the HRR is considered as an important fire reaction property because the heat released can provide additional thermal energy required for the growth and spread of fire [43–45]. It is seen from

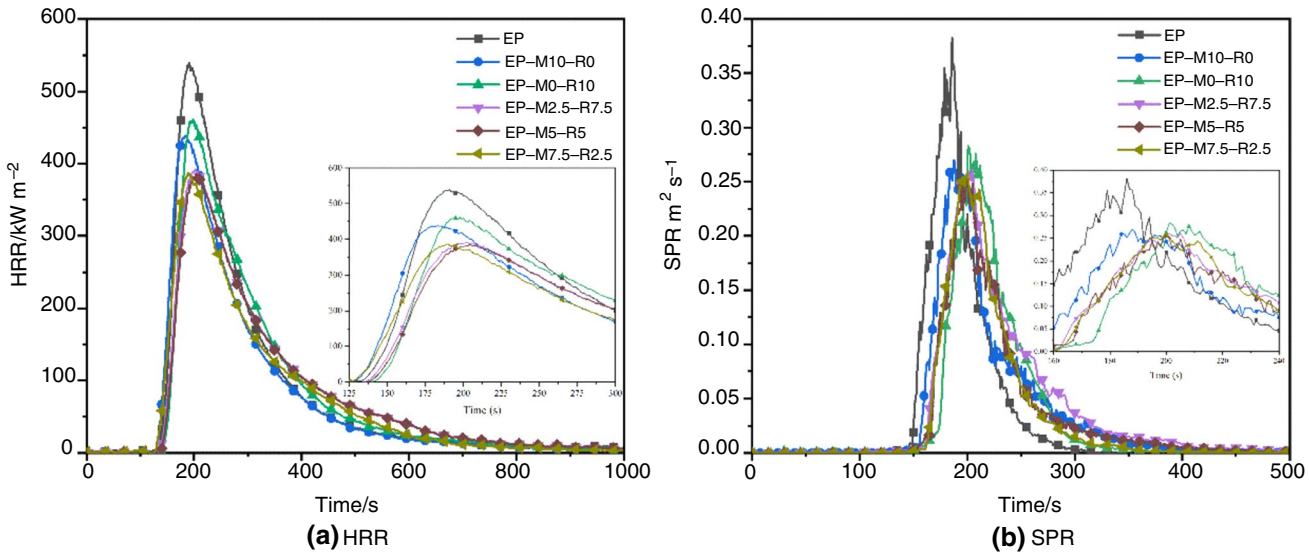

Fig. 4 The curves of HRR and SPR of EP and EP composites

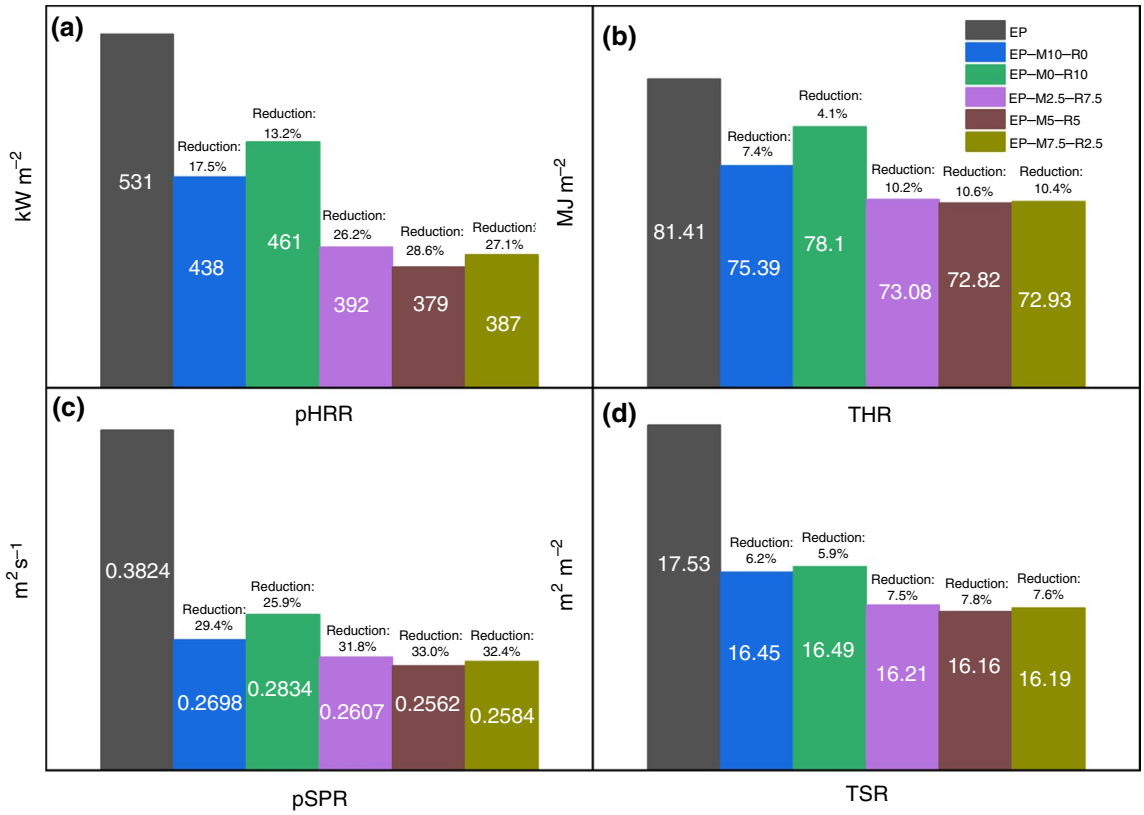

Fig. 5 The value of pHRR, THR, pSPR, TSR, and the rate of reduction compared to EP

Table 3 Cone calorimeter date of EP and EP composites at the irradiance heat flux of 35 kW m^{-2}

Samples	TTI/s	pHRR/kW m^{-2}	THR/MJ m^{-2}	pSPR/m^2 s^{-1}	TSR/m^2 m^{-2}
EP	124	531	81.41	0.3824	17.53
EP-M10-R0	129	438	75.39	0.2698	16.45
EP-M0-R10	140	461	78.10	0.2834	16.49
EP-M2.5-R7.5	138	392	73.08	0.2607	16.21
EP-M5-R5	137	379	72.82	0.2562	16.16
EP-M7.5-R2.5	130	387	72.93	0.2584	16.19

Fig. 5a that in the sample containing 10 mass% Mg-Phyt (EP-M10-R0), the pHRR value is significantly decreased by 17.5%, which indicates that Mg-Phyt could reduce the burning intensity of epoxy resins. In addition, for samples containing both Mg-Phyt and RHS, the pHRR of EP-M2.5-R7.5, EP-M5-R5, and EP-M7.5-R2.5 samples decreased by 26.2%, 28.6%, and 27.1%, respectively. Compared to adding Mg-Phyt or RHS alone, the simultaneous addition of Mg-Phyt and RHS has a synergistic effect on reducing the pHRR. In all tested samples, the pHRR of EP-M5-R5 decreased the most by 28.6%, indicating that when the mass ratio of Mg-Phyt and RHS is 5: 5, the burning intensity can be reduced effectively.

From Fig. 5b, the effect of different flame retardants on the THR of EP samples was similar to those on the pHRR. The THR of EP-M10-R0, EP-M0-R10, EP-M2.5-R7.5, EP-M5-R5, and EP-M7.5-R2.5 samples are decreased by 7.4%, 4.1%, 10.2%, 10.6%, and 10.4%, respectively. It can also be found that compared with pure epoxy resins, the addition of Mg-Phyt reduces THR, indicating that it has a good flame retardant effect on reducing the total fire load. When Mg-Phyt and RHS are added together, the effect on reducing the THR is more obvious due to the synergistic effect. Among all the tested samples, EP-M5-R5 have the lowest pHRR and THR than other formulas.

Figure 5c shows that with the addition of Mg-Phyt, the pSPR value was decreased by 29.4%, compared with pure epoxy resins, which indicates that the smoke suppression effect of Mg-Phyt is good. For the samples containing both Mg-Phyt and RHS, compared with the addition of a single

additive, the pSPR was reduced more. For example, the decrease in the pSPR of EP-M10-R0 was 29.4%, while that of EP-M5-R5 was 33.0%. On the other hand, the addition of Mg-Phyt and RHS reduces TSR (Fig. 5d), the change of TSR was in the range from 5.9% to 7.8%. Therefore, Mg-Phyt and RHS have synergistic effect in reducing pSPR and TSR. Compared with other proportions of Mg-Phyt and RHS, the smoke suppression effect of EP-M5-R5 samples is slightly better.

Figure 6 shows the CO production rate (COP) and CO_2 production rate (CO_2P) during the test. It can be seen that after the addition of Mg-Phyt, the release of CO and CO_2 are decreased. When Mg-Phyt and RHS are added into epoxy resin together, the CO and CO_2 production rates have further declined, suggesting a synergistic effect between Mg-Phyt and RHS to further reduce the toxic gas release. Among all the tested samples, EP-M5-R5 samples have less toxic gas release than other proportions.

In conclusion, the addition of Mg-Phyt can not only reduce the heat release rate and smoke release rate, but also reduce the release amount of CO and CO_2. In addition, when the Mg-Phyt and RHS are added together, each parameter discussed here will be further reduced. Due to the synergistic effect between Mg-Phyt and RHS, the flame retardant effect of EP-M5-R5 is the best.

UL 94 and LOI tests

The flammability of the samples was also evaluated by a UL-94 flame chamber using horizontal test and LOI tests. Table 4 shows the burning rate and LOI value for each sample. The EP burned quickly after ignition and the burning rate was 17.2 mm min^{-1}. With the addition of Mg-Phyt, the burning rate has decreased by 14.5%. It can be seen that the addition of Mg-Phyt can reduce the burning rate of epoxy resins. When Mg-Phyt and RHS were added together to epoxy resins, the burning rate of EP-M2.5-R7.5, EP-M5-R5, and EP-M7.5-R2.5 decreased by 18.0%, 42.4%, and 20.3%, respectively. It can be seen that with the addition of Mg-Phyt and RHS, the burning rate of epoxy resins further slowed down, which indicates that Mg-Phyt and RHS have synergistic effect on reducing the burning rate, and compared with other proportions, the burning rate of EP-M5-R5 samples decreases most.

Table 4 The rate of burning and LOI for each sample

Samples	Rate of burning/ mm min^{-1}	Change in rate of burning/%	LOI/%
EP	17.2	–	21.4
EP-M10-R0	14.7	14.5	22.2
EP-M0-R10	15.5	9.9	23.8
EP-M2.5-R7.5	14.1	18.0	22.9
EP-M5-R5	9.9	42.4	22.1
EP-M7.5-R2.5	13.7	20.3	22.0

For samples containing Mg-Phyt only, LOI value can be increased to 22.2%. When 2.5 mass% Mg-Phyt and 7.5 mass% RHS were added to epoxy resin, LOI value increased to 22.9%, which was higher than LOI value when Mg-Phyt was added alone, but the flame retardant effect was not as good as that when RHS was added alone. Therefore, the addition of RHS is more beneficial to improve LOI value of epoxy resins.

In conclusion, Mg-Phyt can reduce the burning rate and increase the LOI value of epoxy resins to a certain extent.

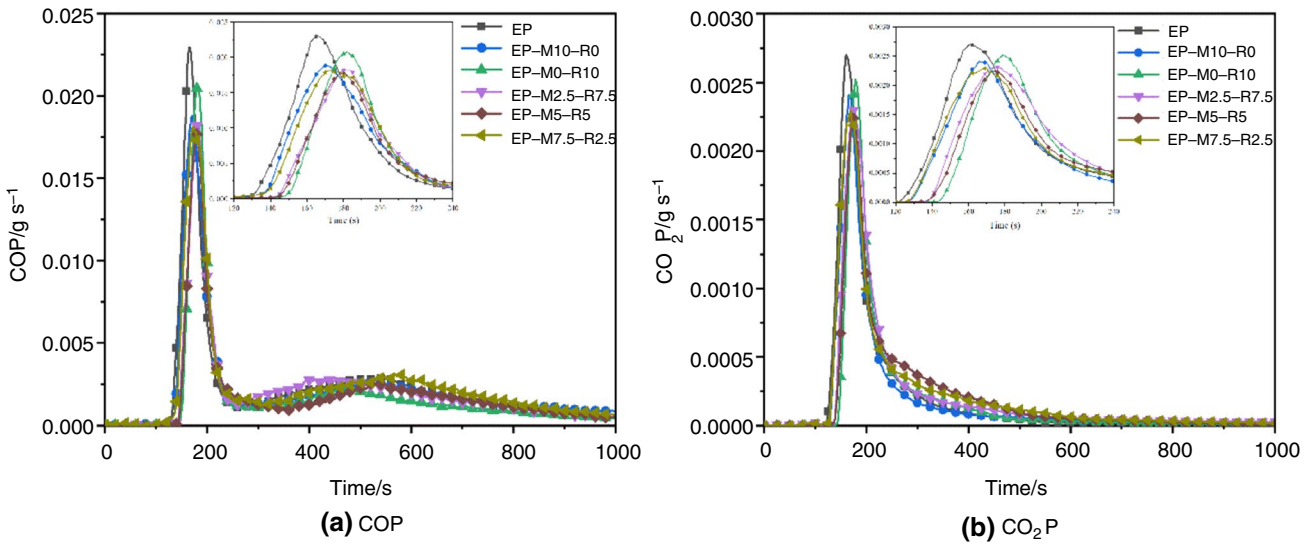

Fig. 6 The curves of COP and CO_2P

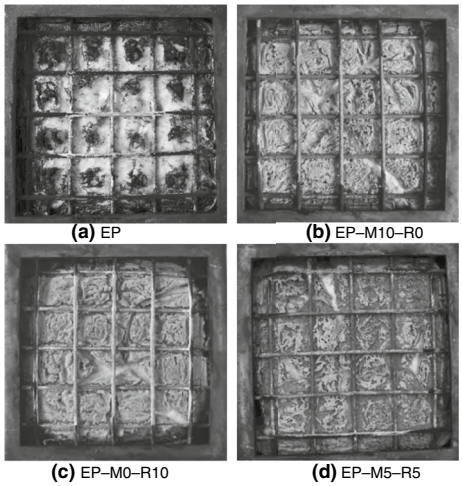

Fig. 7 Digital photographs of chars left after the cone calorimeter test

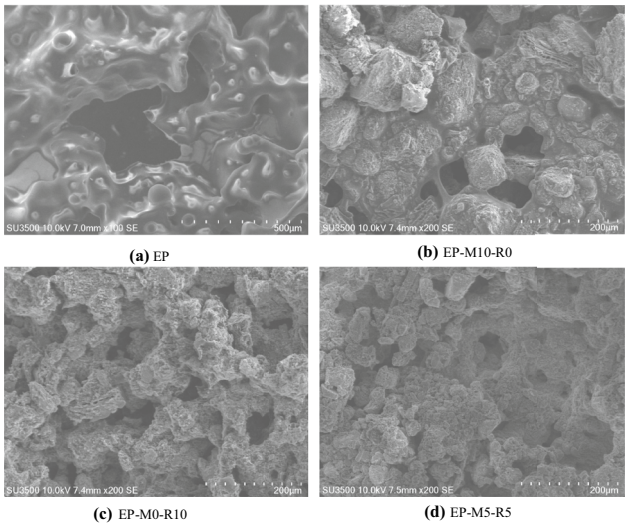

Fig. 8 SEM images of char residues left after the cone

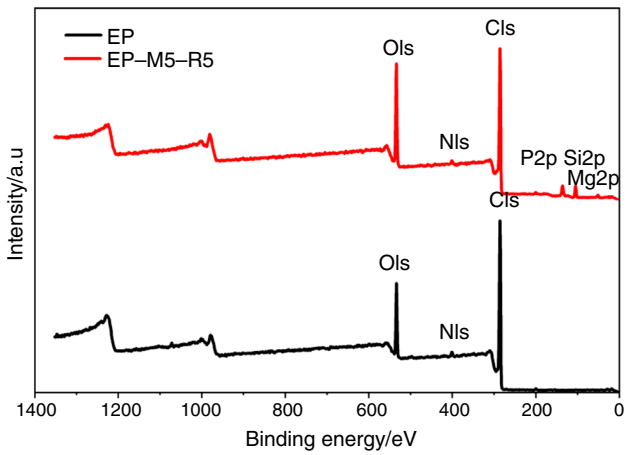

Fig. 9 XPS spectra of char residues of EP and EP-M5-R5

When the Mg-Phyt and RHS are added together, the burning rate is lower, which indicates that the synergism takes place between Mg-Phyt and RHS to reduce the burning rate. When the mass ratio of Mg-Phyt and RHS is 5:5, the burning rate can reach the lowest. RHS has a great influence on LOI value.

Morphology and XPS of the char residues

To understand the flame retardant mechanism, the morphology of char residues was analyzed. Because EP-M5-R5 has the lowest decomposition rate, pHRR, THR, pSPR, TSR, and burning rate in the samples containing both Mg-Phyt and RHS, it was selected for analysis. As a comparison, EP, EP-M10-R0, and EP-M0-R10 were also analyzed. The digital photographs of chars left after the cone calorimeter test of samples are shown in Fig. 7a–d. It can be seen that EP has almost no char residues left, but EP-M10-R0, EP-M0-R10, and EP-M5-R5 all produce a char layer. The char layer of EP-M10-R0 and EP-M0-R10 have large cracks, while the char layer of EP-M5-R5 is more compact and has fewer cracks. The compact char layer is beneficial to prevent heat and mass transfer between flame zone and epoxy resins substrate and thus protect the underlying materials from further pyrolysis. Therefore, the combination of Mg-Phyt and RHS can have a synergistic effect to make the epoxy resins form a better char layer when it is burned.

The char residues were further observed by SEM to compare the structure on the microscopic scale. The SEM images of char residues left after the cone calorimeter test of samples are shown in Fig. 8a–d. It should be noted that due to the large holes on the surface of the EP char residues, the picture with a magnification of 100 times is provided, because if the magnification of 200 times is implemented, only the holes can be observed. Therefore, it can be seen that when the magnification is 100 times, the char residues of EP already have huge holes on the surface which are conducive to the release of smoke and have a negative effect on its flame retardancy. The surface of the char residues of EP-M10-R0, EP-M0-R10 and EP-M5-R5 shows a particulate structure. The accumulated particles on the burning epoxy resins surface slow down the heat and mass transfer between the gaseous and condensed phase and prevent the underlying polymeric substrate from further attacking by heat flux during the combustion process [27]. Compared with EP-M10-R0 and EP-M0-R10, the particles on the surface of EP-M5-R5 are more compact, which means that it has a better effect on preventing heat and mass transfer. This behavior can explain why EP-M5-R5 has the lowest pHRR, THR, pSPR, and TSR.

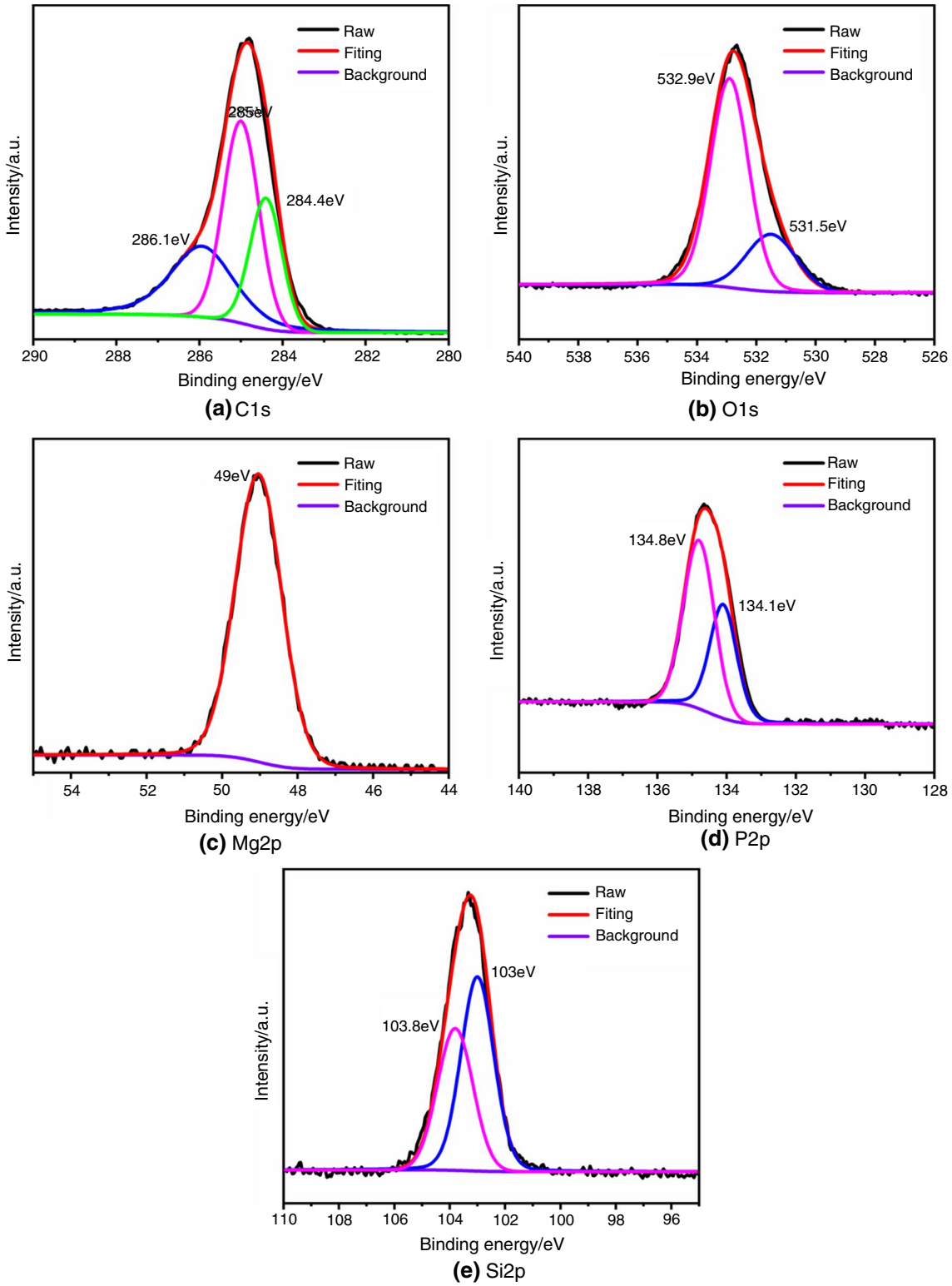

Fig. 10 The XPS spectra of C1s, O1s, Mg2p, P2p, and Si2p of the char residues

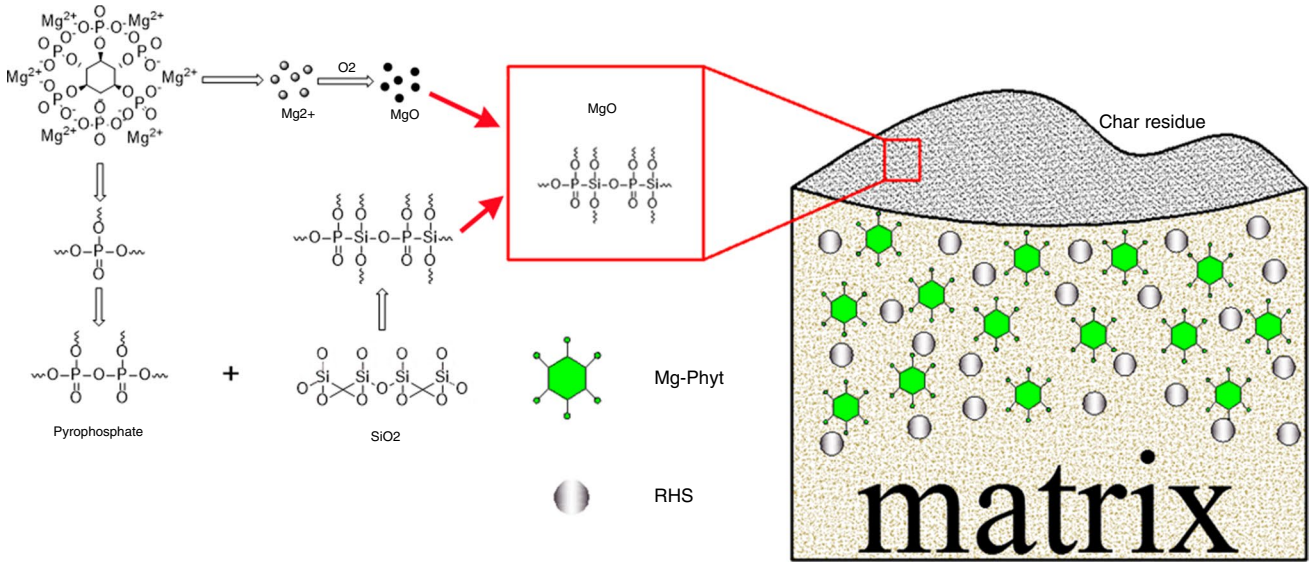

Fig. 11 The proposed synergistic flame retardant mechanism of Mg-Phyt and RHS for epoxy resins

To further explore the synergistic flame retardant mechanism of Mg-Phyt and RHS, XPS was performed to study the chemical structure of char residues of EP and EP-M5-R5. It is seen from Fig. 9 that the char residues of EP are mainly composed of two elements of C and O, while three new elements of P, Si, and Mg appear in the char residues of EP-M5-R5 due to the addition of Mg-Phyt and RHS. These new elements play a flame retardant role in the condensed phase.

The XPS spectra of C1s, O1s, Mg2p, P2p, Si2p of the char residues are shown in Fig. 10a–f. It is seen from Fig. 10a that the C1s peak can be split into three peaks of 284.4 eV, 285 eV, and 286.1 eV, which is attributed to C–H, C–C, and C–O, respectively [46, 47]. Figure 10b shows that there are two peaks in the O1s spectrum, which are 531.5 eV and 532.9 eV. The peak at 531.5 eV is attributed to C=O and –P=O (phosphate), while the peak at 532.9 eV is attributed to the -O- which is from aromatic compounds [47–50]. The peak in Fig. 10c is 49 eV, which is from MgO [51]. As is seen in Fig. 10d, there are two peaks at 134.1 eV and 134.8 eV, which are attributed to the pyrophosphate and P–O–C [52, 53]. Moreover, P–O–C is a thermally stable structure that facilitates the formation of char residues [52]. In the Si2p spectrum in Fig. 10e, the peaks at 103 eV and 103.8 eV are attributed to Si–P and Si–O–Si, respectively [47, 54].

Synergistic flame retardant mechanism

Based on the above results, the possible flame retardant mechanism of Mg-Phyt and RHS is proposed in Fig. 11. When the samples are exposed to a high temperature or high heat flux, Mg-Phyt begins to decompose first. Since Mg-Phyt contains crystalline water, water vapor will be released from the decomposition, which cools and dilutes the combustible gas produced by the decomposition of the epoxy resins. The existence of MgO in char residues indicates that Mg^{2+} produced by the decomposition of Mg-Phyt is oxidized to MgO during the burning. MgO can trap high-energy radicals responsible for flame propagation [55]. XPS analysis shows that –P=O (phosphate) exists in char residue, and phosphate can further form pyrophosphate [47]. The existence of pyrophosphate and Si-P in char residues indicates that the silicon element provided by RHS combines with pyrophosphate to form an integrated and thermally stable char layer containing Si–P structure [47]. Besides, the P–O–C structure with strong thermal stability is also formed in the char layer [27]. The char layer could effectively isolate the heat radiation and help to reduce the decomposition of the epoxy resins matrix. On the other hand, the char layer could prevent the flammable gases from the epoxy resins matrix to the flame zone and impede the combustion of flame. Moreover, silica in RHS has poor heat conduction [56], which also hinders the heat transfer within the epoxy resins substrate. Therefore, both Mg-Phyt and RHS play an essential role in improving the flame retardance of epoxy resins in the condensed phase.

Conclusions

The feasibility of Mg-Phyt as a bio-based phosphorus-containing flame retardant for epoxy resins was studied. The synergistic flame retardant effect of Mg-Phyt and RHS on

epoxy resins was also investigated. The conclusions are as follows:

(1) It is feasible that Mg-Phyt can be used as a bio-based phosphorus-containing flame retardant for epoxy resins. Mg-Phyt could reduce the decomposition rate of the epoxy resins. Furthermore, compared with pure epoxy resins, the pHRR, THR, pSPR, and TSR of epoxy resins with 10 mass% Mg-Phyt (EP-M10-R0) are reduced by 17.5%, 7.4%, 29.4%, and 6.2%, respectively. In addition, Mg-Phyt could reduce the burning rate of epoxy resins and increase LOI value.

(2) Mg-Phyt and RHS have a synergistic flame retardant effect on epoxy resins. The combination of Mg-Phyt and RHS can further decrease the decomposition rate, pHRR, THR, pSPR, TSR, toxic gas release, and burning rate of epoxy resins. When 10 mass% flame retardant was added to the epoxy resins system, 5 mass% Mg-Phyt mixed and 5 mass% RHS had a better synergistic effect on these parameters. The pHRR, THR, pSPR, TSR, and burning rate of epoxy resins with 5 mass% Mg-Phyt and 5 mass% RHS (EP-M5-R5) are reduced by 28.6%, 10.6%, 33.0%, 7.8%, and 42.4%, respectively. It is worth noting that RHS has obvious influence on initial thermal decomposition temperature ($T_{5\%}$), the maximum thermal decomposition temperature (T_{max}), time to ignition (TTI) and LOI of epoxy resins. With the increase in RHS content, the above four parameters all increase.

(3) Mg-Phyt and RHS have a synergistic effect on char formation, which can help to form a silica-rich char layer containing Si–P and P–O–C structures with strong thermal stability to hinder the heat transfer into the epoxy resins substrate and reduce flammable gas emission. Therefore, the flame retardancy of epoxy resins can be further improved.

Acknowledgements This work was financially supported by the Scientific Research Project of Liaoning Provincial Department of Education (JYT19065), and Natural Science Foundation of Liaoning Province (No. 20180540033).

References

1. Yan L, Xu Z, Deng N, Chu Z. Synergistic effects of mono-component intumescent flame retardant grafted with carbon black on flame retardancy and smoke suppression properties of epoxy resins. J Therm Anal Calorim. 2019;138(2):915–27.
2. Liu L, Xu Y, Xu M, Li Z, Hu Y, Li B. Economical and facile synthesis of a highly efficient flame retardant for simultaneous improvement of fire retardancy, smoke suppression and moisture resistance of epoxy resins. Compos Part B Eng. 2019;167:422–33.
3. Mariappan T, Wilkie J. Flame retardant epoxy resin for electrical and electronic applications. Fire Mater. 2014;38:588–98.
4. Anurag Y, Amit K, Kamal S, Manoj KS. Investigating the effects of amine functionalized graphene on the mechanical properties of epoxy nanocomposites. Mater Today. 2019;11:837–42.
5. Song Q, Wu H, Liu H, Han X, Qu H, Xu J. Synergistic flame-retardant effects of ammonium polyphosphate and AC-Fe_2O_3 in epoxy resin. J Therm Anal Calorim. 2019;138(2):1259–67.
6. Zhang Y, Yu B, Wang B, Liew KM, Song L, Wang C, Hu Y. Highly effective P-P synergy of a novel DOPO-based flame retardant for epoxy resin. Ind Eng Chem Res. 2017;56:1245–55.
7. Lu S, Hamerton I. Recent developments in the chemistry of halogen-free flame retardant polymers. Prog Polym Sci. 2002;27:1661–712.
8. Ma C, Yu B, Hong N, Pan Y, Hu W, Hu Y. Facile synthesis of a highly efficient, halogen-free, and intumescent flame retardant for epoxy resins: thermal properties, combustion behaviors, and flame-retardant mechanisms. Ind Eng Chem Res. 2016;55:10868–79.
9. Rakotomalala M, Wagner S, Doring M. Recent developments in halogen free flame retardants for epoxy resins for electrical and electronic applications. Materials. 2010;3:4300–27.
10. Schartel B. Phosphorus-based flame retardancy mechanisms-old hat or a starting point for future development? Materials. 2010;3:4710–45.
11. Qin ZL, Li D, Yang R. Study on inorganic modified ammonium polyphosphate with precipitation method and its effect in flame retardant polypropylene. Polym Degrad Stab. 2016;126:117–24.
12. Cheng X, Shi W. Synthesis and thermal properties of silicon-containing epoxy resin used for UV-curable flame-retardant coatings. J Therm Anal Calorim. 2011;103(1):303–10.
13. Murat S, Dilem S, Dogan M. Comparative study of boron compounds and aluminum trihydroxide as flame retardant additives in epoxy resin. Polym Adv Technol. 2014;25:769–76.
14. Zhang JH, Kong QH, Wang DY. Simultaneously improving the fire safety and mechanical properties of epoxy resin with Fe-CNTs via large-scale preparation. J Mater Chem A. 2018;6(15):6376–86.
15. Ding JM, Zhang Y, Zhang X, Kong QH, Zhang JH, Liu H, Zhang F. Improving the flame-retardant efficiency of layered double hydroxide with disodium phenylphosphate for epoxy resin. J Therm Anal Calorim. 2020;140(1):149–56.
16. Kong QH, Wu T, Zhang HK, Zhang Y, Zhang MM, Si TY, Yang L, Zhang JH. Improving flame retardancy of IFR/PP composites through the synergistic effect of organic montmorillonite intercalation cobalt hydroxides modified by acidified chitosan. Appl Clay Sci. 2017;146:230–7.
17. Qian L, Qiu Y, Wang J, Wang X. High-performance flame retardancy by char-cage hindering and free radical quenching effects in epoxy thermosets. Polymer. 2015;68:262–9.
18. Yang S, Zhang Q, Hu Y. Synthesis of a novel flame retardant containing phosphorus, nitrogen and boron and its application in flame-retardant epoxy resin. Polym Degrad Stab. 2016;133:358–66.
19. Kong QH, Sun YL, Zhang CJ, Guan HM, Zhang JH, Wang DY, Zhang F. Ultrathin iron phenyl phosphonate nanosheets with appropriate thermal stability for improving fire safety in epoxy. Compos Sci Technol. 2019;182:107748.
20. Ren H, Sun J, Wu B, Zhou Q. Synthesis and properties of a phosphorus-containing flame retardant epoxy resin based on bisphenoxy (3-hydroxy) phenyl phosphine oxide. Polym Degrad Stab. 2007;92:956–61.
21. Alexander S, Sebastian S, Wiebke L, Olaf W, Manfred D. Synthesis and properties of flame-retardant epoxy resins based on DOPO and one of its analog DPPO. J Appl Polym Sci. 2008;105:685–96.
22. Perret B, Schartel B, Stoss K, Ciesielski M, Diederichs J, Doring M, Krämer J, Altstädt V. Novel DOPO-based flame retardants in

high-performance carbon fibre epoxy composites for aviation. Eur Polym J. 2011;47:1081–9.
23. Salmeia KA, Gaan SJ. An overview of some recent advances in DOPO derivatives: chemistry and flame retardant applications. Polym Degrad Stab. 2015;113:119–34.
24. Zhao C, Li Y, Xing Y, He D, Yue J. Flame retardant and mechanical properties of epoxy composites containing APP-PSt core-shell microspheres. Appl Polym Sci. 2014;131(9):40218.
25. Tan Y, Shao Z, Yu L, Xu Y, Rao W, Chen L, Wang Y. Polyethyleneimine modified ammonium polyphosphate toward polyamine-hardener for epoxy resin: thermal stability, flame retardance and smoke suppression. Polym Degrad Stab. 2016;131:62–70.
26. Zhang Z, Ma Z, Leng Q, Wang Y. Eco-friendly flame retardant coating deposited on cotton fabrics from bio-based chitosan, phytic acid and divalent metal ions. Int J Biol Macromol. 2019;140:303–10.
27. Yang W, Tawiah B, Yu C, Qian Y, Wang L, Yuen ACY, Zhu SE, Hu EZ, Chen TBY, Yu B, Lu H. Manufacturing, mechanical and flame retardant properties of poly(lactic acid) biocomposites based on calcium magnesium phytate and carbon nanotubes. Compos Part A Appl Sci Manuf. 2018;110:227–36.
28. Cheng L, Wu W, Meng W, Xu S, Han H, Yu Y, Qu H, Xu J. Application of metallic phytates to poly(vinyl chloride) as efficient biobased phosphorous flame retardants. J Appl Polym Sci. 2018;135(33):46601.
29. Costesab L, Laoutida F, Dumazertc L, José-Marie L, Sylvain B, Christian D, Philippe D. Metallic phytates as efficient bio-based phosphorous flame retardant additives for poly(lactic acid). Polym Degrad Stab. 2015;119:217–27.
30. Attia NF, Lee SM, Kim HJ, Geckeler KE. Nanoporous carbon-templated silica nanoparticles: preparation, effect of different carbon precursors, and their hydrogen storage adsorption. Microporous Mesoporous Mater. 2013;173:139–46.
31. Saraswathy V, Hawon S. Corrosion performance of rice husk ash blended concrete. Constr Build Mater. 2007;21:1779–84.
32. Arora S, Kumar M, Kumar M. Preparation and thermal stability of poly(methyl methacrylate)/rice husk silica/triphenylphosphine nanocomposites: assessment of degradation mechanism using model-free kinetics. J Compos Mater. 2012;47:2027–38.
33. Almiron J, Roudet F, Duquesne S. Influence of volcanic ash, rice husk ash, and solid residue of catalytic pyrolysis on the flame-retardant properties of polypropylene composites. J Fire Sci. 2019;37:434–51.
34. Wu W, He H, Liu T, Wei R, Cao X, Sun Q, Venkatesh. Synergetic enhancement on flame retardancy by melamine phosphate modified lignin in rice husk ash filled P34HB biocomposites. Compos Sci Technol. 2018;168:246–54.
35. Liu Y, Chiu Y, Wu C. Preparation of silicon-/phosphorous-containing epoxy resins from the fusion process to bring a synergistic effect on improving the resins' thermal stability and flame retardancy. J Appl Polym Sci. 2003;87(3):404–11.
36. He Z, Wayne H, Zhang T, Paul MB. Preparation and FT-IR characterization of metal phytate compounds. J Environ Qual. 2006;35:1319–28.
37. Xue Z, Zhang Y, Li G, Wang J, Zhao W, Mu T. Niobium phytate prepared from phytic acid and $NbCl_5$: a highly efficient and heterogeneous acid catalyst. Catal Sci Technol. 2016;6:1070–6.
38. Sun P, Li Z, Song M, Wang S, Yin X, Wang Y. Preparation and characterization of zirconium phytate as a novel solid intermediate temperature proton conductor. Mater Lett. 2017;191:161–4.
39. Xu Y, Sun X, Shen R, Wang Z, Wang Q. Thermal behavior and smoke characteristics of glass/epoxy laminate and its foam core sandwich composite. J Therm Anal Calorim. 2020;141(3):1173–82.
40. Nour FA, Heshiam AA, Mohamed AH. Synergistic study of carbon nanotubes, rice husk ash and flame retardant materials on the flammability of polystyrene nanocomposites. Mater Today. 2015;2:3998–4005.
41. Liu Y, Wei W, Hsu KY, Ho WH. Thermal stability of epoxy-silica hybrid materials by thermogravimetric analysis. Thermochim Acta. 2004;412(1–2):139–47.
42. Shen R, Hatanaka LC, Ahmed L, Agnew RJ, Mannan MS, Wang Q. Cone calorimeter analysis of flame retardant poly(methyl methacrylate)-silica nanocomposites. J Therm Anal Calorim. 2017;128(3):1443–51.
43. Ahmed L, Zhang B, Shen R, Agnew RJ, Park H, Cheng Z, Mannan MS, Wang Q. Fire reaction properties of polystyrene-based nanocomposites using nanosilica and nanoclay as additives in cone calorimeter test. J Therm Anal Calorim. 2018;132(3):1853–65.
44. Xu Y, Lv C, Shen R, Wang Z, Wang Q. Experimental investigation of thermal properties and fire behavior of carbon/epoxy laminate and its foam core sandwich composite. J Therm Anal Calorim. 2019;136(3):1237–47.
45. Xu Y, Lv C, Shen R, Wang Z, Wang Q. Comparison of thermal and fire properties of carbon/epoxy laminate composites manufactured using two forming processes. Polym Compos. 2020;9(41):3778–86.
46. Zheng Z, Liu S, Wang B, Yang T, Cui X, Wang H. Preparation of a novel phosphorus- and nitrogen-containing flame retardant and its synergistic effect in the intumescent flame-retarding polypropylene system. Polym Compos. 2015;36:1606–19.
47. Chen Z, Jiang M, Chen Z, Chen T, Yu Y, Jiang J. Preparation and characterization of a microencapsulated flame retardant and its flame-retardant mechanism in unsaturated polyester resins. Powder Technol. 2019;354:71–81.
48. Zhao C, Liu Y, Wang D, Wang D, Wang Y. Synergistic effect of ammonium polyphosphate and layered double hydroxide on flame retardant properties of poly(vinyl alcohol). Polym Degrad Stab. 2008;93:1323–31.
49. Bettina D, Karen AW, Daniel H, Rolf M, Bernhard S. Flame retardancy through carbon nanomaterials: carbon black, multiwall nanotubes, expanded graphite, multi-layer graphene and graphene in polypropylene. Polym Degrad Stab. 2013;98:1495–505.
50. Liu Y, Zhao J, Deng C, Chen L, Wang D, Wang Y. Flame-retardant effect of sepiolite on an intumescent flame-retardant polypropylene system. Ind Eng Chem Res. 2011;50:2047–54.
51. Chen J, Zhu J. A query on the Mg 2p binding energy of MgO. Res Chem Intermed. 2019;45:947–50.
52. Gao Y, Deng C, Du Y, Huang S, Wang Y. A novel bio-based flame retardant for polypropylene from phytic acid. Polym Degrad Stab. 2019;161:298–308.
53. Feng C, Liang M, Zhang Y, Jiang J, Huang J, Liu H. Synergistic effect of lanthanum oxide on the flame retardant properties and mechanism of an intumescent flame retardant PLA composites. J Anal Appl Pyrol. 2016;122:241–8.
54. Chen W, Liu Y, Liu Y, Wang Q. Preparation of alginate flame retardant containing P and Si and its flame retardancy in epoxy resin. J Appl Polym Sci. 2017;134(48):45552.
55. Richard HT, Artur W, Luke H. Fire retardant action of mineral fillers. Polym Degrad Stab. 2011;96:1462–9.
56. Baine P, Khor YC, Gamble HS, Armstrong BM, Mitchell SJN. Novel materials for thermal via incorporation into SOI structures. J Mater Sci Mater Eectron. 2001;12:215–8.